Available online at www.sciencedirect.com
ScienceDirect
Nuclear Physics B Proceedings Supplement 00 (2012) 1–6
Nuclear Physics B Proceedings Supplement

Heavy Flavour Production at HERA

Kenan Mujkic,
University College London (UCL) and Deutsches Elektronen Synchrotron (DESY)
On behalf of the H1 and ZEUS collaborations

Abstract

Measurements of heavy-quark production at HERA constrain the structure of the proton, and have provided valuable vindications of perturbative QCD. In this publication measurements of heavy-flavour jet cross sections in photoproduction and deep inelastic scattering (DIS), performed by the H1 and ZEUS collaborations, are presented using inclusive techniques for the signal extraction. The results are compared to next-to-leading order QCD calculations and found to be in reasonable agreement with theory predictions.

Keywords:

This proceeding reviews inclusive measurements of heavy-flavour production at HERA in photoproduction and deep inelastic scattering (DIS) performed by the H1 and ZEUS collaborations. The study of beauty and charm production in ep collision constitutes a stringent test of perturbative Quantum Chromo Dynamics (QCD), since the heavy-quark masses provide a hard scale, thereby allowing precise predictions to be made [1]. At leading order, the dominant process for heavy quark production at HERA is boson-gluon fusion (BGF), $\gamma g \rightarrow q\bar{q}$ with $q \in \{b, c\}$. The massive quarks are generated in the hard sub-process, and next-to-leading-order (NLO) QCD calculations are expected to provide reliable predictions for heavy-quark jet production cross sections.

Provided the negative squared four-momentum exchanged at the electron vertex, Q^2, is small, the scattering process can be treated as photoproduction, where a quasi-real photon emitted by the incoming electron interacts with the proton. In this proceeding a measurement of heavy-quark jet cross sections in photoproduction will be presented, which is based upon the semileptonic decay of heavy-flavoured hadrons into muons, and which uses the signed impact parameter δ and the relative transverse momentum P_T^{rel} of the muon to the heavy-quark jet axis as variables for the signal extraction. The measured heavy-quark jet cross sections are compared to NLO QCD predictions and previous measurements using exclusive tagging techniques. Furthermore, a measurement of heavy-flavour jet cross sections based upon the decay length significance of the decaying hadrons and the invariant mass of the tracks associated to the decay vertex will be presented. The results are compared to NLO QCD predictions.

In the case of large momentum transfer, Q^2, between the electron vertex and a constituent of the proton, usually referred to as deep inelastic scattering (DIS), the production of heavy flavours is of particular interest for testing pQCD calculations, since the process involves two hard scales: the square root of the photon virtuality Q^2 and the heavy quark mass $m_{b/c}$. In the final section of this proceeding inclusive measurements of heavy-quark jet cross sections in deep inelastic scattering will be presented. The results will be compared to NLO QCD predictions, and the charm contribution $F_2^{c\bar{c}}$ to proton structure function will be extracted.

1. Photoproduction

Beauty and charm has been measured in photoproduction using various techniques by both the ZEUS and

H1 collaborations. In the measurements presented in this publication the cross sections have been determined using semi-leptonic decays into muons, and the decay length significance and secondary vertex mass of decaying charm and beauty hadrons. In the muon analysis performed by the H1 collaboration, the fraction of leptons originating from beauty was determined using the large transverse momentum of the muon relative to the axis of the associated jet, P_T^{rel}, and the impact parameter of the muons. The inclusive analysis performed by the ZEUS collaboration relies upon the reconstruction of secondary vertices of decaying hadrons and uses two discriminating variables, the significance of the reconstructed decay length and the invariant mass of the charged tracks associated with the secondary vertex.

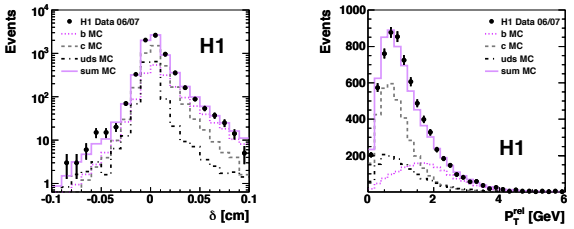

Figure 1: Signed impact parameter δ and relative transverse momentum P_T^{rel} of muon μ.

The muon analysis performed by the H1 collaboration to measure beauty and charm cross sections requires events with two jets and a muon, where the muon is associated with one of the jets. The analysis exploits the lifetime and the mass of heavy flavoured hadrons. Compared to previous measurements, a more precise test of pQCD predictions was possible due to increased statistics, an extended phase space and reduced systematics due to an improved understanding of the H1 vertex detector.

The identification of muon candidates relies upon a combination of information from the central silicon tracker (CST) and the central tracking detector (CTD). At least two CST hits in the $r-\phi$ plane have to be associated with the muon track, and the track segments must be well matched to a track reconstructed in the CTD. Jets are reconstructed using the inclusive longitudinally invariant k_T algorithm in the massless P_T recombination scheme, with the distance parameter $R_0 = 1$ in the $\eta - \phi$ plane [2]. The algorithm is applied in the laboratory frame using all reconstructed hadronic final state particles including the muon candidate. A jet is defined as a μ-jet if the selected muon candidate lies within a cone of radius 1 about the jet axis in the $\eta - \phi$ plane.

The signal to background separation is performed exploiting the properties of the muon track associated to the μ-jet [3]. The impact parameter δ of a muon track is the transverse distance of closest approach (DCA) of the muon track to the beam spot point. In case the angle α between the azimuthal angle of the μ-jet and the line joining the primary vertex to the point of closest approach is less than 90°, the impact parameter is defined as positive. It is defined negative otherwise. The transverse momentum P_T^{rel} of the muon relative to the μ-jet axis is also sensitive to the quark content of the event sample and used together with the impact parameter for the flavour separation. The distributions used for the flavour separation are shown in figure 1.

The fractions of events with beauty, charm and light quarks are obtained by a binned likelihood fit in the $\delta - P_T^{rel}$ plane [4]. In order to extract the differential cross sections the fit is performed separately for each individual differential bin, while the total cross sections are determined using the fractions obtained from a fit to the complete event sample.

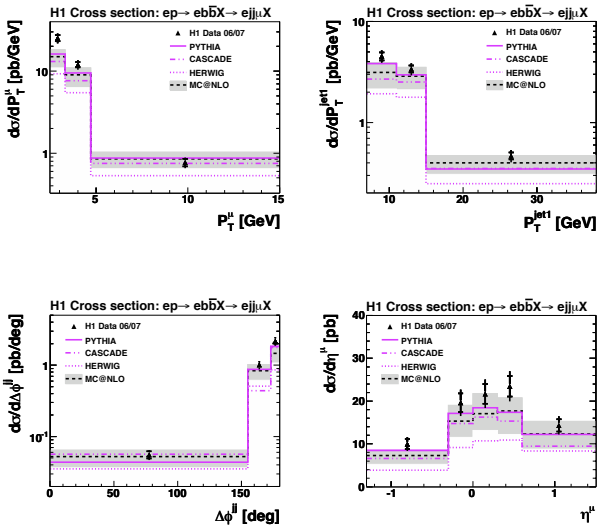

Figure 2: Differential cross sections as function of transverse momentum P_T^{jet1} of leading jet, transverse momentum P_T^{μ} and pseudorapidity η^{μ} of muon μ and azimuthal angular difference $\Delta\phi^{ij}$.

The beauty and charm cross sections are measured differentially as a function of the transverse momentum P_T^{jet1} of the leading jet, the transverse momentum P_T^{μ} and the pseudorapidity η^{μ} of the muon and the azimuthal angular difference $\Delta\phi^{ij}$ between the two leading jets. The results are presented in figure 2 [5] and compared to next-to-leading order (NLO) calculations provided by MC@NLO [6], a program calculating next-to-leading order QCD predictions in the massive fixed

flavour number scheme (FFNS). In general the predictions are in reasonable agreement with the beauty and charm measurements.

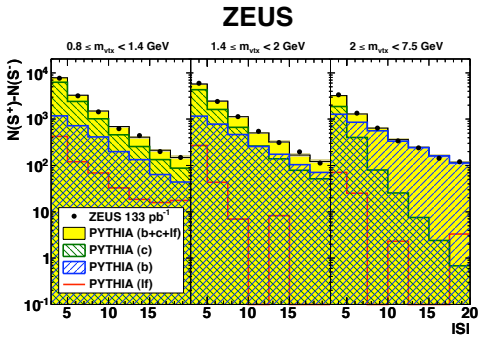

Figure 3: Mirrored and subtracted decay length significance distributions $S^+ - S^-$ in bins of the secondary vertex mass M_{vtx}.

The inclusive analysis performed by the ZEUS collaboration measured beauty and charm quarks with at least two jets using the invariant mass of charged tracks associated with secondary vertices and the decay length significance of these vertices [7]. In this context the decay length, d, was defined as the distance in $X - Y$ between the secondary vertex and the interaction point, projected onto the jet axis in the $X - Y$ plane. The sign of the decay length was assigned using the axis of the jet to which the vertex is associated. In case the decay-length vector was in the same hemisphere as the jet axis, a positive sign was assigned to it; otherwise the sign of the decay length was negative. The decay length significance, S, is defined as $d/\delta d$, where δd is the uncertainty on d.

The shape of the decay-length significance distribution together with the secondary-vertex mass distribution, m_{vtx}, was used to extract the beauty and charm content. The invariant mass of the tracks fitted to the secondary vertex provides a distinguishing variable for jets from beauty and charm quarks, reflecting the different masses of the beauty and charm hadrons. Aiming to minimise the effect of the light-flavour contribution, the contents of the negative bin of the significance distribution, $N(S^-)$, were subtracted from the contents of the corresponding positive bin, $N(S^+)$, resulting in a subtracted decay-length significance distribution shown in figure 3.

In order to reduce the uncertainty due to remaining differences between data and MC in the core region of the significance distribution, a cut of $|S| > 3$ was applied. The beauty and charm contributions were then extracted using a least-squares fit to the subtracted distributions in the three mass bins. The MC beauty, charm and light-flavour contributions, normalised to the data luminosity, were scaled by the factors k_b, k_c and k_{lf} to give the best fit to the observed subtracted distributions. In order to extract the differential cross sections the fitting procedure was repeated for every differential bin.

Parton-level jets were found by applying the k_T cluster algorithm to the generated partonic final state. The NLO QCD predictions for the parton-level jets were corrected for hadronisation effects applying a bin-by-bin procedure, where $d\sigma = d\sigma_{NLO} \cdot C_{had}$ and $d\sigma_{NLO}$ is the cross section for partons in the final state of the NLO calculation. The hadronisation-correction factors, C_{had} were obtained from the ratio of the hadron-level to the parton-level MC jet cross section. In this context the parton level is defined as the result of the parton-showering stage of the simulation.

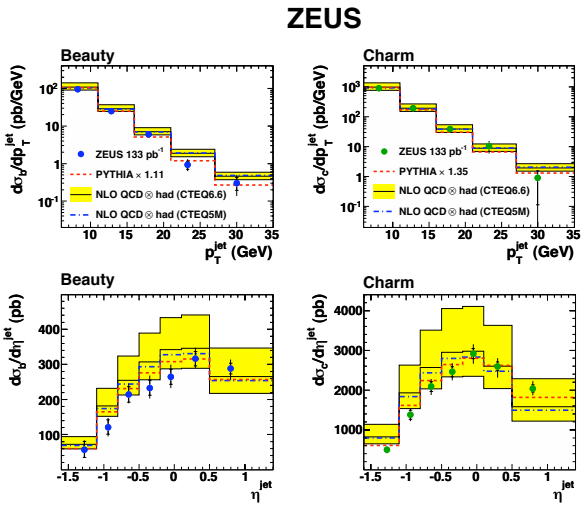

Figure 4: Differential beauty and charm jet cross sections as function of transverse momentum p_T^{jet} and pseudo-rapidity η^{jet}.

Finally, inclusive beauty and charm cross section have been measured as functions of the transverse momentum, p_T^{jet}, and the pseudo-rapidity, η^{jet}, of the jet, and compared to NLO QCD predictions generated with the FMNR program [8]. The NLO calculations were based on the fixed-flavour-number scheme, using three light flavours for charm predictions and four flavours for beauty predictions. In order to allow for comparison with previous measurements the PDFs were taken from CTEQ6.6 [9] for the proton and GRV-G HO [10] for the photon. The heavy-quark masses were set to $m_b = 4.75$ GeV and $m_c = 1.5$ GeV, and the QCD scale, Λ_{QCD}, to

0.226 GeV. The renormalization scale, μ_R, and the factorisation scale, μ_F, were chosen to be equal and set to $\mu_R = \mu_F = \frac{1}{2}(\hat{p}_T^2 + m_{b(c)}^2)^{\frac{1}{2}}$, where $\hat{p}_T$ is the average transverse momentum of the heavy quarks.

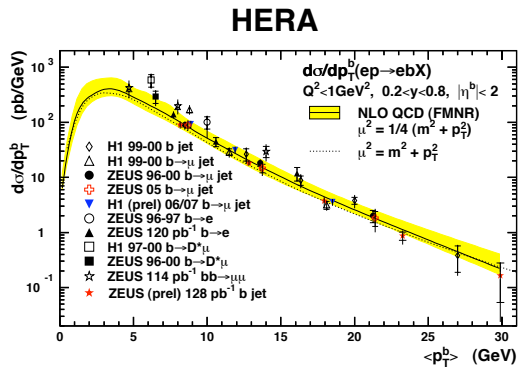

Figure 5: Differential beauty jet cross sections as function of average transverse momentum p_T^b of the b-quark.

The results are shown in figure 4 and 5 [7]. In general a good agreement between the measured beauty and charm cross sections and the NLO predictions is observed. Compared to previous measurements of specific decay chains, this analysis has increased statistics and reduced the uncertainty originating from the branching fractions. Furthermore, the measurement presented in this proceeding extends the kinematic region to higher p_T^b values than previous measurements and represents the most precise measurement of b-quark photoproduction at HERA.

2. Deep Inelastic Scattering

The measurement of beauty and charm jet cross sections in DIS at HERA performed by the H1 collaboration uses an inclusive lifetime technique to distinguish jets containing beauty and charm flavoured hadrons from those containing light flavoured hadrons only [11]. The most important of these inputs are the transverse displacement of tracks from the primary vertex and the reconstructed position of a secondary vertex in the transverse plane. Typically, heavy flavoured hadrons have longer life times than light flavoured hadrons and therefore produce tracks with a significant displacement from the primary vertex. For jets with three or more tracks in the vertex detector the reconstructed variables are used as input to a neural network to discriminate beauty from charm events.

In the analysis presented in this proceeding the flavour of the event is defined as the flavour of the jet with the highest transverse energy, E_T^{jet}, in the laboratory frame. The separation of beauty, charm and light flavour jets is performed using the properties of tracks within a cone of radius 1 from the jet axis in the $\eta - \phi$ plane [2]. The tracks are reconstructed in the CTD, must have at least 2 CST hits and transverse momentum greater than 300 MeV. The signed impact parameter δ is defined as the distance of closest approach of the track to the beam spot. Tracks with $\delta > 0.1$ cm are rejected to suppress contributions from decays of long-lived strange particles.

The track significance S is defined as $S = \delta/\sigma(\delta)$, where $\sigma(\delta)$ is the uncertainty on the signed impact parameter δ. The tracks are ordered according to their absolute track significance, and the sign of the highest absolute significance track is used as reference. In the track selection the remaining tracks will only be considered, if they have the same sign like the highest significance track. The significances S_1, S_2 and S_3 are then defined as the significance of the track with the highest, second highest and third highest absolute significance after the described track selection. The number of tracks in the jet after this selection is called N_{track}, and the selected tracks are also used to reconstruct the position of the secondary vertex associated with the jet.

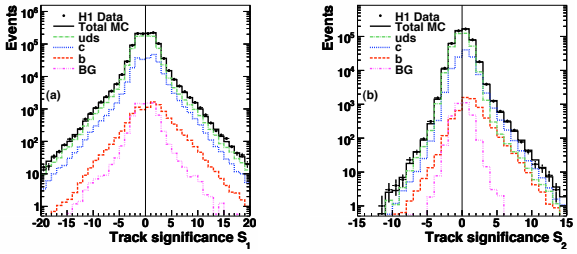

Figure 6: Highest and second highest track significance after selection of jet associated tracks.

In order to obtain statistically independent distributions for the signal extraction, the jets are separated into three independent samples. For each sample a different distribution is used to separate the beauty, charm and light flavour jets. The S_1 distribution is used for jets, where only one track has passed the cuts, and the S_2 distribution for jets, where two tracks have passed the cuts. For jets with $N_{track} \geq 3$, where S_1, S_2 and S_3 all have the same sign an artificial neural network (NN) is used to produce a distribution that combines several variables in order to provide an optimal discrimination between beauty and charm jets.

The input to the NN are S_1, S_2, S_3, the significance of the transverse distance between the secondary and pri-

mary vertex, the transverse momenta of the tracks with the highest and second highest transverse momentum, N_{track}, and the number of reconstructed tracks at the secondary vertex [11]. The NN is trained using a sample of inclusive heavy flavour DIS Monte Carlo events, with beauty events as "signal" and charm events as "background". The output of the neural network is signed according to the sign of S_1.

Given that the S_1, S_2 and NN output distributions for light flavour jets are nearly symmetric around zero the sensitivity to the modelling of the light jets can be reduced by subtracting the contents of the negative bins from the contents of the corresponding positive bins. The subtracted distributions are dominated by beauty and charm jets, and the fraction of events with charm, beauty and light jets is extracted using a least squares simultaneous fit to the subtracted S_1, S_2 and NN output distributions and the total number of events after DIS and jet selection.

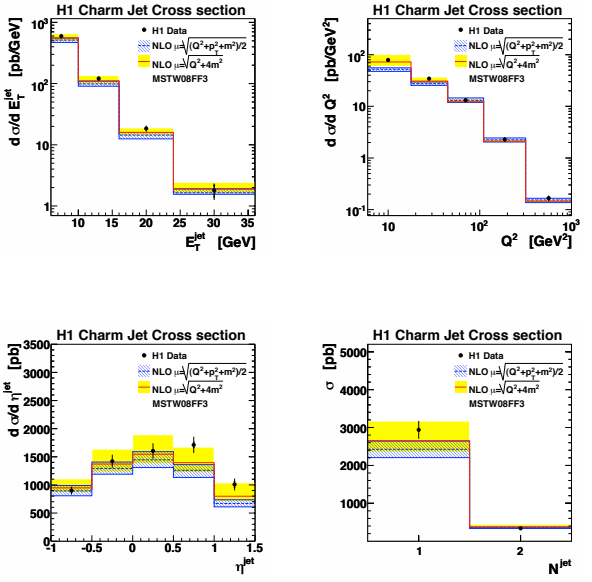

Figure 7: Differential charm jet cross sections as function of transverse energy E_T^{jet}, photon virtuality Q^2, pseudo-rapidity η^{jet} and number of tracks N_{track}.

Differential charm and beauty jet cross sections were measured as a function of E_T^{jet}, η^{jet}, Q^2 and N^{jet}. The measured cross sections have been compared to NLO QCD predictions generated with the HVQDIS program [12]. The predictions are based on a fixed flavour number scheme (FFNS) which uses the massive PGF $O(\alpha_s^2)$ matrix element [13] and provides weighted events with two or three partons, i.e. a heavy quark pair and possibly an additional light parton.

In order to investigate the dependence of the NLO predictions on the renormalisation and factorisation scale two different choices for the scale have been made. Firstly, the scale $\mu_r = \mu_f = \sqrt{(Q^2 + p_T^2 + m_{c/b}^2/2}$ was used, where p_T is the highest heavy quark transverse momentum in the virtual photon-parton centre of mass frame. This choice of scale was motivated by the comparison of NLO QCD predictions with recent measurements of inclusive jet data by the H1 collaboration. Secondly, the scale $\mu_r = \mu_f = \sqrt{Q^2 + 4m^2}$ was chosen, which has been used previously in the comparison of HVQDIS predictions with H1 inclusive and dijet D^* DIS data [14], [15].

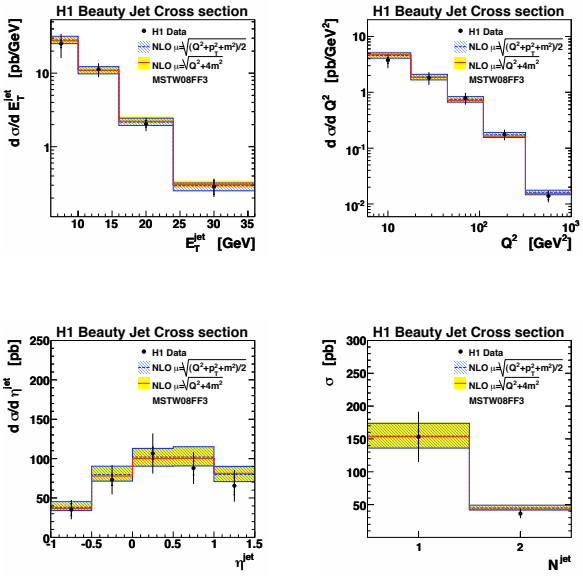

Figure 8: Differential beauty jet cross sections as function of transverse energy E_T^{jet}, photon virtuality Q^2, pseudo-rapidity η^{jet} and number of tracks N_{track}.

The charm cross sections are shown in figure 7 together with the NLO predictions generated with the HVQDIS [11] program that is based on the fixed-flavour-number scheme (FFNS), in which the heavy quarks are produced in the interaction. In general the NLO predictions describe the data reasonably well in all differential distributions, although the predictions generated with the first renormalisation and factorisation scale fall somewhat below the data at low Q^2, low E_T^{jet} and in the forward η^{jet} region. On the other hand, the differential beauty jet cross sections presented in figure 8 are in reasonable agreement with NLO predictions with little dependence on the choice of scale.

The inclusive measurement of charm jet cross sections in deep inelastic scattering performed by the

ZEUS collaboration uses the same technique like the measurement in photoproduction, and relies upon the significance of the reconstructed decay length and the invariant mass of the charged tracks associated to the decay vertex. The measurement is kept fully inclusive aiming to extract the heavy quark content to the proton structure function with high precision.

For this purpose differential cross sections as functions of the photon virtuality Q^2 and the Bjoerken scaling variable x have been measured. The results were compared to NLO QCD predictions and the heavy-quark contribution to the proton structure function was extracted. Theory predictions were obtained from the HVQDIS program using ZEUS-S [16] and ABKM as proton PDFs, and setting the value of the strong coupling constant $\alpha_S(M_Z) = 0.118$ and the heavy-quark masses $m_c = 1.5$ GeV and $m_b = 4.75$ GeV. The renormalisation and factorisation scale were chosen to be equal and set to $\mu_r = \mu_f = \sqrt{Q^2 + 4m^2_{c/b}}$.

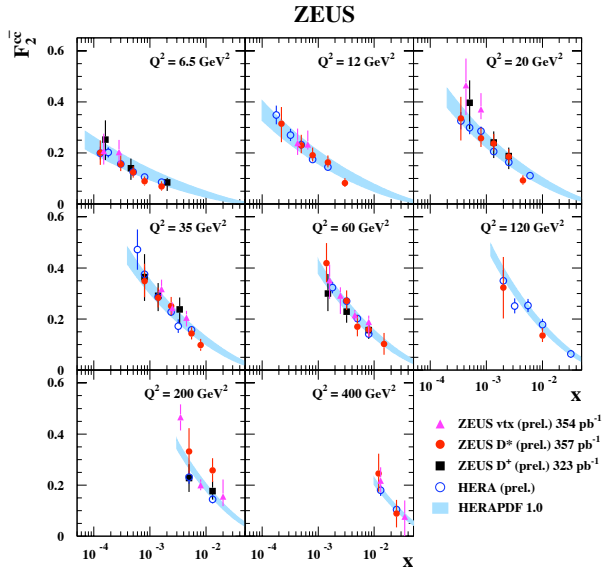

Figure 9: Charm contribution $F_2^{c\bar{c}}$ to the proton structure function as function of Bjoerken x in various bins of Q^2.

The heavy quark contribution to the proton structure function can be defined in terms of an inclusive double-differential cross section:

$$\frac{d^2\sigma_{q\bar{q}}}{dx\,dQ^2} = \frac{2\pi\alpha^2_{em}}{xQ^4}\{\{1+(1-y^2)F_2^{q\bar{q}}(x,Q^2) - y^2F_L^{q\bar{q}}(x,Q^2)\}\},$$

where $F_L^{q\bar{q}}$ is the heavy-quark contribution to the structure functions F_L.

In order to extract $F_2^{q\bar{q}}$ from the visible cross sections, $\sigma_{q\bar{q}}$, an extrapolation from the measured range in E_T^{jet} and η^{jet} to the full phase space was performed. The measured values of $F_2^{q\bar{q}}$ at a reference point in the $x-Q^2$ plane were calculated using

$$F_2^{q\bar{q}}(x,Q^2) = \frac{d^2\sigma_{q\bar{q}}}{dx\,dQ^2} \cdot \frac{F_2^{q\bar{q},NLO}(x,Q^2)}{d^2\sigma^{NLO}_{q\bar{q}}/dx\,dQ^2} \quad ,$$

where $F_2^{q\bar{q},NLO}$ and $d^2\sigma^{NLO}_{q\bar{q}}/dx\,dQ^2$ were calculated at NLO in the FFNS using the HVQDIS program corrected for hadronisation and QED radiation effects.

The charm contribution $F_2^{c\bar{c}}$ to the proton structure function extracted in this way is shown in figure 9 as a function of x for various values of Q^2. The measurement is compared to the NLO QCD predictions generated with HVQDIS and HERAPDF 1.0, and found to be in agreement with theoretical predictions within the statistical and systematic uncertainties. The measurement is in agreement with the HERA combined measurements and particularly competitive at high Q^2.

References

[1] S. Frixione, P. Nason and G. Ridolfi, Nucl. Phys. **B 454** 3 (1995). S. Frixione *et al.*, Phys. Lett. **B 348** 633 (1995).
[2] S. D. Ellis and D. E. Soper, Phys. Rev. **D48** (1993) 3160. S. Catani, Y. L. Dokshitzer, M. H. Seymour, and B. R. Webber, Nucl. Phys. **B406** (1993) 187.
[3] A. Aktas *et al.*, Eur. Phys. J **C41** (2005) 453.
[4] R. J. Barlow and C. Beeston, Comput. Phys. Commun. **77** (1993) 219.
[5] F. D. Aaron *et al.*, Eur. Phys. J. **C72**, 2047 (2012).
[6] S. Frixione, P. Nason and B. R. Webber, JHEP 1101 (2011) 053.
[7] H. Abramowicz *et al.*, Eur. Phys. J. **C71**, 1659 (2011).
[8] F. Frixione *et al.*, Nucl. Phys. **B 412**, 225 (1994).
[9] J. Pumplin *et al.*, JHEP **07**, 012 (2002).
[10] M. Glück, E. Reya and A. Vogt, Phys. Rev. **D 46**, 1873 (1992). M. Glück, E. Reya and A. Vogt, Phys. Rev. **D 45**, 3986 (1992).
[11] F. D. Aaron *et al.*, Eur. Phys. J. **C71**, 1509 (2011).
[12] B. W. Harris and J. Smith, Phys. Rev. **D 57**, 2806 (1998). B. W. Harris and J. Smith, Phys. Rev. **B 452**, 109 (1995). B. W. Harris and J. Smith, Phys. Rev. **B 353**, 535 (1995).
[13] E. Laenen, S. Riemersma, J. Smith and W. L. van Neerven, Nucl. Phys. B **392** (1993) 162. E. Laenen, S. Riemersma, J. Smith and W. L. van Neerven, Nucl. Phys. B **392** (1993) 229.
[14] C. Adloff *et al.*, Phys. Lett. B **528** (2002) 199. F. D. Aaron *et al.*, Phys. Lett. B **686** (2010) 91.
[15] A. Aktas *et al.*, Eur. Phys. J **C51** (2007) 271.
[16] S. Chekanov *et al.*, Phys. Rev. **D 67**, 012007 (2003).